Modeling of the Thermal Conductivity of U-Mo/Al Dispersion Fuel

Byoung Jin Cho

Department of Nuclear Engineering
Graduate School of UNIST

2015

Modeling of the Thermal Conductivity of U-Mo/Al Dispersion Fuel

A thesis
submitted to the Graduate School of UNIST
in partial fulfillment of the
requirements for the degree of
Master of Science

Byoung Jin Cho

01. 16. 2015

Approved by

Advisor
Prof. Dong Seong SOHN

Co-Advisor
Dr. Yeon Soo Kim

Modeling of the Thermal Conductivity of U-Mo/Al Dispersion Fuel

Byoung Jin Cho

This certifies that the thesis of Byoung Jin Cho is approved.

01. 16. 2015

Advisor: Prof. Dong Seong Sohn

Prof. Ji Hyun Kim: Thesis Committee Member

Prof. In Cheol Bang: Thesis Committee Member

Abstract

Thermal conductivity of U-Mo/Al dispersion fuel was empirically modeled. The modeling expanded one of the most widely accepted theoretical models for a composite material, the Bruggeman model.

The Bruggeman model, as other theoretical models commonly do, assumes perfect contact between the fuel particles and Al matrix and also assumes the Al matrix is a defect-free monolithic continuum. However, it is known that the U-Mo particle surface has a thin oxide layer, so the contact between the U-Mo and Al is partial. The Al matrix is also made of Al powder, which makes the Al matrix a thermally imperfect medium. Because of these factors, the theoretical model predicts substantially higher than the measured. In addition, the theoretical model lacks a capability to consider the effect of fuel particle size.

The newly developed model considers thermal resistances at the interfaces between the U-Mo and Al and the Al-Al interfaces, which were expressed as a function of U-Mo particle size and Al particle size, respectively, and empirically obtained by data fitting of measured data available in the literature.

Contents

1. Introduction 1

1.1 General Background 1

1.2 The objectives and scope of this study 2

2. Theoretical Models 3

2.1 Ohm's Law 3

2.2 Maxwell Model 5

2.3 Bruggeman Model 6

2.4 Hasselman and Johnson Model 6

3. Measured Data 7

3.1 Measured Data of Lee et al. 8

3.2 Measured Data of R.E. Taylor 11

3.3 Comparison of the measured data of U-Mo/Al dispersion fuel 12

3.4 Thermal conductivity of U-Mo 13

3.5 Thermal conductivity of Aluminum 17

3.6 Comparison of data by S.H. Lee and predictions by Bruggeman model 18

4. Analysis of the data 20

4.1 Al thermal conductivity 20

4.2 Analysis of measured data by S.H. Lee 22

4.2.1 Review of preparation 22

4.2.2 Density correction 22

5. New Thermal Conductivity Model for U-Mo/Al Dispersion Fuel 23

5.1 Modeling of thermal conductivity of pure Al 23

5.2 Correction of density employed by S.H. Lee 24

5.2.1 Thermal expansion and density of Aluminum 24

5.2.2 Thermal expansion and density of U-Mo 26

5.2.3 Densities of U-Mo/Al dispersion fuel 26

5.3 Comparison of density-corrected Lee data and predicted thermal conductivity 29

5.4 Sample homogeneity 32

5.5 Comparison of density-corrected average Lee data and predictions of Bruggeman model 36

5.6 Interfacial thermal resistance between U-Mo and Al 37

5.7 Al-Al interfacial resistance 39

5.8 New model 41

5.9 Comparison of density-corrected average Lee data and predictions of new model 43

6. Sensitivity Study 44

7. Conclusions 46

References 47

Acknowledgments 49

1. Introduction

1.1 General Background

U-Mo alloy fuel is a promising candidate for conversion of high-power research and test reactors thanks to its higher uranium densities and stable irradiation performance. Two forms of U-Mo alloy fuel have were developed under the auspices of the US Reduced Enrichment in Research and Test Reactors (RERTR) program and other programs. One form is a monolithic form, in which a solid U-Mo fuel foil is directly bonded to aluminum cladding. The other is U-Mo particle dispersion in an Al matrix (U-Mo/Al dispersion fuel). The fueled zone where U-Mo particles are dispersed throughout the Al matrix is referred as the fuel core or fuel meat in the dispersion fuel. In this dissertation, we focused only on the dispersion fuel form because modeling the thermal conductivity of meat in U-Mo/Al dispersion fuel was concerned.

Evaluation of the fuel meat thermal conductivity is the most important element of calculating meat temperature distribution. Fuel meat thermal conductivity is essentially dependent on local fuel morphology and material composition. However, very few studies have been published on investigating meat thermal conductivity since it has been difficult to quantify fuel meat thermal conductivity experimentally due to the challenges from local heterogeneity of fuel particles in meat samples. Lee [1] obtained the thermal conductivities of dispersion fuel meat samples in the temperature range of 25 – 380 ℃ using the measured thermal diffusivity, specific heat capacity and density.

The multiphase conductivity models derived by different authors [2-4] have been employed to calculate the meat thermal conductivity due to those difficulties in the experiment. The meat was regarded as a two phase material from purely theoretical considerations that Al matrix constitutes one phase, and the fuel particle constitutes the other.

When we compared meat thermal conductivities measured by Lee and the predicted by the multiphase model, a significant discrepancy was found. We noticed that meat density used to determine meat thermal conductivity was likely to be independent to the experimental temperature, which was not reasonable. This is also believed due to theoretical assumptions in the model such as no thermal interfacial resistances, or a perfect contact among two different constituents.

In this study, we focused on correction of measured meat thermal by Lee, modifying of the meat thermal conductivity prediction model, and comparing those two data.

1.2 The objectives and scope of this study

In the present study, we corrected the meat thermal density by introducing temperature-dependent densities of U-Mo fuel and Al matrix.

This thesis also focuses on modifying multiphase model to calculate meat thermal conductivity. In the model used, the contribution of new factors for interfacial resistances of each constituent was to take into account. Finally, the measured data with the correction and predicted meat thermal conductivity were compared in order to assess the effect of those factors on the meat thermal conductivity.

Since the measured meat thermal conductivity was in out-of-pile conditions, we did not attempt to examine the effect of interaction layer on meat thermal conductivity as it is beyond the scope of the present study.

Until now, there is no example of thermal conductivity modelling about U-Mo/Al dispersion fuel. Several organizations have used the original theoretical models. These models were not verified enough so there is possibility that they are wrong. In this situation, the results of this study are expected to complement the original models. Furthermore, they can be used to verify a great amount of future data.

2. Theoretical Models

2.1 Ohm's Law

Lots of models have been developed over the last century to predict the thermal conductivity of two-phase composites for which a dispersion of a second phase in a continuous medium of the first phase is assumed. The models either assume or require as input a specific dispersion of second phase, and these have been reviewed by a number of authors. The models have been applied solid-liquid, solid-gas and solid-solid composite systems.

The simplest cases based on the Ohm's law are the series, parallel and geometric mean models, for which the conductivity of the composite is given by [5] :

Parallel $$k_e = k_1 V_1 + k_2 V_2 \tag{2.1}$$

Series $$k_e = \frac{k_1 k_2}{V_2 k_1 + V_1 k_2} \tag{2.2}$$

Geometric Mean $$k_e = k_1^{V_1} k_2^{V_2} \tag{2.3}$$

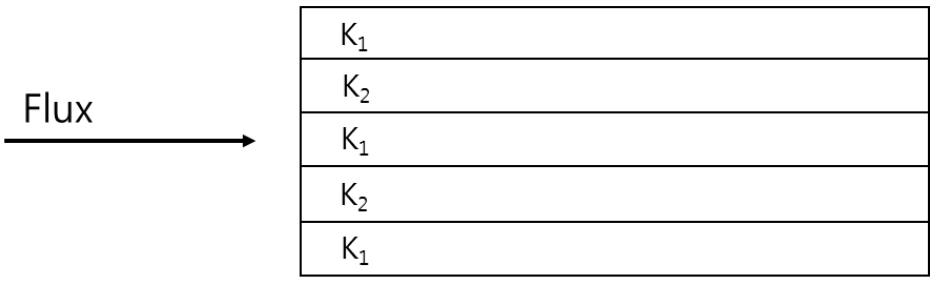

Fig. 1 Parallel distribution case.

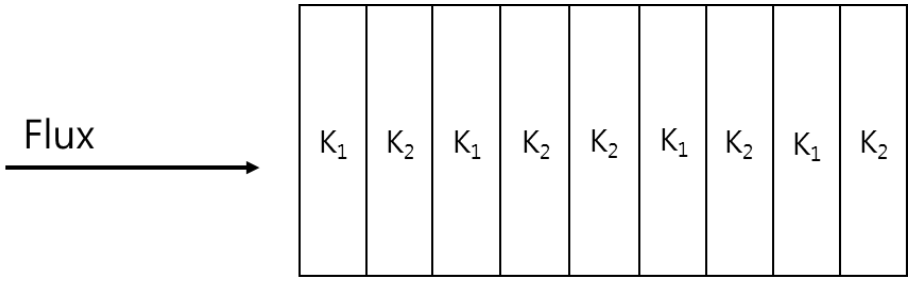

Fig. 2 Series distribution case.

In the derivation of Ohm's law of equations, it is assumed that the lines of flux are straight. Actually, the flow lines will not be straight, but will bend toward or away from the discontinuous particle depending on its conductivity relative to that of the surrounding medium [6].

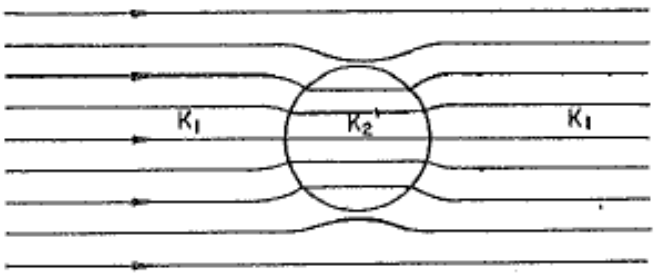

Fig. 3 Flux Lines for Particle 2 in Medium 1.

2.2 Maxwell Model

Historically, more sophisticated heat transfer models may be classified as either flux law models, where the temperature field is solved for an assumed geometry, or Ohm's law models based on an electrical series resistance analogy. The earliest flux law is that of Maxwell, who considered cube of a suspension containing a single particle. The derived equation is [2]:

$$k_e = k_m \left[\frac{2k_m + k_p - 2V_p\left(k_m - k_p\right)}{2k_m + k_p + V_p\left(k_m - k_p\right)} \right] \tag{2.4}$$

Maxwell model has the following assumptions :

1) the dispersed particles are spherical,

2) the particles are non-interacting,

3) the interfacial resistance between the two phases is negligible.

This model is only applicable for low particle concentration because of the assumptions made in the derivation of this model.

2.3 Bruggeman Model

Because of the limitations of the Maxwell model, Bruggeman in 1935 devised an alternative means of extending Maxwell model by considering an infinite number of small additions to a homogeneous mixture of the two phases. For a two-phase system containing a uniformly round shaped second phase dispersion, Bruggeman is expressed as [3]:

$$k = \frac{1}{4}\left[A + \left(A^2 + 8k_1k_2 \right)^{\frac{1}{2}} \right], A = \left(3\nu_1 - 1 \right)k_1 + \left(3\nu_2 - 1 \right)k_2 \tag{2.5}$$

2.4 Hasselman and Johnson Model

Hasselman and Johnson also modified Maxwell's calculation to derive a new expression for the effective thermal conductivity of composites containing spherical, cylindrical, and flat plate second-phase particles. They found that the effective thermal conductivity is not only dependent on the volume fraction of second-phase particles but also on the size of dispersed particles. This result is because the interfacial thermal resistance increases with the decreasing size of the dispersed particles due to the larger interfacial area. They obtained expressions for composites containing spherical and cylindrical dispersed particles by modifying the original Maxwell equation. The effective thermal conductivity of composites is expressed as [7] :

$$k_{eff} = k_m \frac{2\left(\frac{k_p}{k_m} - \frac{k_p}{ah_c} - 1 \right)v_p + \frac{k_p}{k_m} + 2\frac{k_p}{ah_c} + 2}{\left(1 - \frac{k_p}{k_m} + \frac{k_p}{ah_c} \right)v_p + \frac{k_p}{k_m} + 2\frac{k_p}{ah_c} + 2} \tag{2.6}$$

Where α is the radius of particle and h_c is the interfacial thermal conductance. Hasselman and Johnson introduced the interfacial thermal conductance and considered the effect of particle size on the effective thermal conductivity.

3. Measured Data

Data for thermal conductivity of U-Mo/Al fuel are scarce. There are only two sets of data which are Lee et al. [1] and R.E. Taylor [8].

In general, thermal conductivity is calculated with the experimentally measured specific heat capacity, thermal diffusivity, and density.

$$\lambda = \rho \alpha C_p \tag{3.1}$$

Where,

λ = Thermal Conductivity

ρ = Bulk Density

α = Thermal Diffusivity

C_p = Specific Heat Capacity

The specific heat capacity is measured with a differential scanning calorimeter (DSC). Thermal diffusivity is determined using the laser flash diffusivity method.

3.1 Measured Data of Lee et al.

Uranium molybdenum powder was fabricated by a centrifugal atomized method. The molybdenum-to-uranium ratios were 6, 8, and 10 weight% to produce the initial powder, which was then combined with aluminum (Al 1060). The volume fractions of U–Mo powder to aluminum were 10, 30, 40, and 50vol. % to fabricate the dispersion fuel. The thermal diffusivity and specific heat capacity were measured by the laser-flash and differential scanning calorimetry (DSC) methods, respectively. Densities were measured using the Archimedes method at room temperature. Thermal conductivities were computed by Eq. (3.1). Lee's results were shown in Tables 2 – 4. Although the thermal diffusivity showed a decreasing trend with the U–Mo volume fraction when the dispersion quantity was insignificant, the trend reversed with a higher dispersion level. The specific heat capacity increases monotonically with temperature; its value is larger for a smaller dispersion level. Additionally, the overall thermal conductivity increases with temperature. Finally, the thermal conductivity decreases with an increase in the amount of U–Mo powder in the dispersion fuel.

Table 1 Samples of U-Mo/Al Dispersion Fuel Meats

Sample ID	Sample description	U-Mo (vol.% meat)	Density ($g \cdot cm^{-3}$)			Thermal conductivity [c] (W/m·K)
			DSC [a]	LF [b]	Theoretical	
U10M_A10	U-10 weight% Mo/Al atomized method	10	3.69	4.12	4.13	197.2
U10M_A30		30	7.08	7.00	7.00	128.7
U10M_A40		40	8.71	8.69	8.43	96.5
U10M_A50		50	9.85	9.80	9.86	73.0
U8M_A10	U-8 weight% Mo/Al atomized method	10	4.16	4.16	4.17	180.3
U8M_A30		30	7.27	7.15	7.10	124.2
U8M_A40		40	9.36	9.20	8.56	93.9
U8M_A50		50	10.81	10.54	10.03	66.8
U6M_A10	U-6 weight% Mo/Al atomized method	10	4.23	4.19	4.20	183.1
U6M_A30		30	7.30	7.22	7.20	131.3
U6M_A40		40	8.68	8.76	8.70	107.5
U6M_A50		50	10.20	10.26	10.21	82.5

[a] DSC : samples for specific heat capacity measurements.

[b] LF : samples for thermal diffusivity measurements.

[c] Room temperature values.

Table 2 Thermal conductivity of U-10 weight% Mo/Al Dispersion Fuel Fabricated by Atomized Method

Temp (℃)	U10M_A10	U10M_A30	U10M_A40	U10M_A50
25	197.2	128.7	96.5	73
50	200.5	130.8	98.6	73.7
100	205.8	134.5	102.2	75.7
150	209.7	137.7	105.2	78.3
200	212.2	140.3	107.7	81.4
250	213.7	142.6	109.9	84.9
300	214.1	144.4	112	88.6
350	213.8	146	114.1	92.4
380	213.3	146.7	115.5	94.6

Table 3 Thermal conductivity of U-8 weight% Mo/Al Dispersion Fuel Fabricated by Atomized Method

Temp (℃)	U8M_A10	U8M_A30	U8M_A40	U8M_A50
25	180.3	124.2	93.9	66.8
50	183.4	127	95.8	68.6
100	187.8	131.6	99.5	72.1
150	190.4	135.1	102.7	75.1
200	191.8	137.6	105.6	77.7
250	192.6	139	108	80.1
300	193.4	139.3	110	82.2
350	194.6	138.8	111.5	84.2
380	195.9	138.1	112.3	85.3

Table 4 Thermal conductivity of U-6 weight% Mo/Al Dispersion Fuel Fabricated by Atomized Method

Temp (℃)	U6M_A10	U6M_A30	U6M_A40	U6M_A50
25	183.1	131.3	107.5	82.5
50	186.8	134.8	110	83.4
100	192.7	141	114.6	85.8
150	196.9	145.9	118.8	88.7
200	199.6	149.5	122.3	91.9
250	200.8	151.6	125.1	95
300	200.6	152.2	127.1	97.8
350	199.2	151.5	128.3	100
380	197.9	150.4	128.6	100.8

3.2 Measured Data of R.E. Taylor

Samples of U-10 Mo alloy embedded in an aluminum matrix and clad with 6061 aluminum were submitted for thermal conductivity determinations. U-10 Mo alloy was fabricated by mechanical grinding method.

Thermal diffusivity (α) was measured using the laser flash technique. Bulk density (ρ) values were calculated from the sample's geometries and masses. Specific heat (C_p) values were measured using a differential scanning calorimeter and thermal conductivity (λ) values were calculated as a product of the above Eq. (3.1).

Density and specific heat values for the core materials were furnished by Argonne National Laboratory. The density values for the cores were reported to be 10.06 and 8.29 gm cm^{-3} for TP2 and TP3, respectively.

Thermal conductivity values for the cores are given in Table 5. Along with Lee's measured data, the overall thermal conductivity increases with temperature.

Table 5 Thermal conductivity of U-10 weight% Mo/Al Dispersion Fuel

Temp (℃)	TP2-6	TP2-7	TP3-6	TP3-7
23	66.5	65.1	103.9	74
50	68.2	70.7	103.6	77
100	70.9	77.8	106.8	82.1
200	87.1	83.1	105.1	105.1
300	90.9	87.3	115.9	114.7
400	98.5	93.2	131.4	128.2
500	100.1	93.3	124.9	124.8

3.3 Comparison of the measured data of U-Mo/Al dispersion fuel

Measured data of Lee and Taylor were arranged in Table 6. Lee's data has various range of Mo weight fraction and volume fraction of U-Mo particles and sample was made by atomization fabrication method. This study was conducted with Lee's data.

Table 6 Summary of Measured Data

Author	Year	Particles	Volume Fraction	Temperature Range	Thermal Conductivity	U-Mo particle Frabrication Method
S.H. Lee et al.	2007	U-10wt.%Mo	10 %	25 – 380 ℃	197.2–241.1	Atomization method
			30 %		128.7–146.7	
			40 %		96.5–115.5	
			50 %		73.0–94.6	
		U-8wt.%Mo	10 %		180.3–195.9	
			30 %		124.2–139.3	
			40 %		93.9–112.3	
			50 %		66.8–85.3	
		U-6wt.%Mo	10 %		183.1–200.8	
			30 %		131.3–150.4	
			40 %		107.5–128.6	
			50 %		82.5–100.8	
R.E. Taylor	2000	U-10wt.%Mo	40 %	23 – 500 ℃	65.8–96.7	Mechanical grinding method
			50 %		89.0–129.8	

3.4 Thermal conductivity of U-Mo

Thermal conductivity data as a function of temperature are available from several references [9-19]. Data are listed in Table 7, and plotted in Fig. 4. From the plot, it is apparent that the data of Konobeevsky [12] are not in accord with the data from other sources, so these data are not used in developing a correlation for thermal conductivity. The effect of varying alloy content within the range of 6-10 wt. % (likely to be used for U-Mo dispersions) is probably negligible in comparison to the scatter in the data. The simple linear fit shown by Eq. (3.2) thus provides an approximate representation of the data.

$$k_{U-Mo} \approx 0.037T + 2 \qquad (298 \le T \le 773\ \mathrm{K}) \qquad (3.2)$$

Here $k_{U\text{-}Mo}$ is in units of $W \cdot m^{-1}K^{-1}$ and T is absolute temperature.

Table 7 Thermal conductivity data for U-Mo Alloys. [9]

Comp. (wt.%)	Temp. (℃)	Thermal Conductivity ($W \cdot m^{-1}K^{-1}$)	Reference
U-5Mo	127	22.1	[10, 19]
	177	22.8	
	227	23.8	
	277	24.2	
	327	24.9	
	377	25.6	
	427	26.9	
	477	28.2	
	527	29.5	
U-8Mo	10-100	14.2	[13]
U-9Mo	100	16.7	[12]
	200	20.9	
	300	26.8	
	400	32.6	
	500	38.5	
U-9.2Mo	20	14.3	[14]
	100	16.6	
	200	19.4	
	300	22.3	
	400	25.1	
	500	27.9	
	600	31.1	
U-10Mo	23	12.1	[11]
	100	14.2	

	200 300 400 500 600 700 800 1000	14.2 17.2 20.1 23.0 26.4 30.1 33.9 37.7	
U-10Mo	25 100 200 300 400 500	9.7 11.7 14.0 17.2 21.6 25.7	[15]
U-10Mo	20 100 200 300 400 500 600	12.1 13.8 17.3 20.1 23.3 27.2 30.1	[19]
U-10Mo	50 212 308 404	12.97+1.26 17.99+2.52 21.34+2.52 25.94+4.18	[16]
U-10.7Mo	20 100 200 300 400 500 600	11.9 14.4 17.5 20.6 23.7 26.9 26.9	[17]
U-12Mo	10-100	13.8	[13]

The correlation given in Eq. (3.2) gives a rule-of-thumb estimate for thermal conductivity neglecting the effective of Mo content in the alloy. However, when a more accurate correlation for the effect of the Mo content is needed, the modeling described below is useful.

Touloukian et al. [19] summarized the thermal conductivity data for uranium metal available before 1970. The only data accumulated since then were by Takahashi et al. [18]. For the temperature range $255 \leq T \leq 1173$ K, the thermal conductivity increased monotonically as temperature increased. A parabolic function of temperature was used to fit the data for U-10Mo. Consequently, the thermal conductivity of uranium metal takes the form

$$k_U(T) = 21.73 + 1.591 \times 10^{-2} T + 5.907 \times 10^{-6} T^2 \tag{3.3}$$

Where k is the thermal conductivity in $W \cdot m^{-1}K^{-1}$ and T the temperature in K. The temperature range for Eq. (3.3) was $255 \leq T \leq 1173$ K.

For the thermal conductivity of Mo metal, Touloukian et al. [19] tabulated the recommended values based on assessment of data in the literature. The recommended values showed that the thermal conductivity of Mo decreased linearly as temperature increased for the temperature range of $300 \leq T \leq 800$ K. A linear function of temperature was selected to fit the data. By fitting the data, the thermal conductivity of U-10Mo was obtained as

$$k_{Mo}(T) = 150.0 - 4.0 \times 10^{-2} T \tag{3.4}$$

Where T is in the range of $300 \leq T \leq 800$ K.

Thermal conductivity data of U-Mo alloy are available from Refs. 7 - 16 for the Mo content range of 5 - 12 wt. %. The U-Mo system has the second-phase metallic compound, U2Mo, at 300 - 800 K, which approximately corresponds to U-17Mo. At this composition, the alloy would have the lowest thermal conductivity. However, because no data were available for the composition and a more conservative approach was deemed necessary, we assumed that the thermal conductivity reached its minimum at 29 wt. % Mo in the alloy. Since no data for U-29Mo were available, U-29Zr data were adopted among U-based alloys with available thermal conductivity [10]. By fitting the data accumulated and prepared above to the following correlation, the thermal conductivity of unirradiated U-Mo fuel was modeled

$$k^0_{U-Mo} = (1 - \sqrt{1 - x_{Mo}})k_{Mo} + \sqrt{1 - x_{Mo}} \left\{ (1 - x_{Mo}) k_U + x_{Mo} k_{c,Mo} \right\} \tag{3.5}$$

Where k^0_{U-Mo} is in $W \cdot m^{-1}K^{-1}$, x_{Mo} is the Mo content in weight fraction. k_U is given by Eq. (3.3), and k_{Mo} by Eq. (3.4). $k_{c,Mo}$ is a result of the regression analysis of the data to Eq. (3.5) and takes the form

$$\begin{aligned} k_{c,Mo} = {} & -274.4 + 985.2 x_{Mo} - 1.941 \times 10^3 x_{Mo}^{\ 2} + 3.640 \times 10^{-2} T + \\ & 7.365 \times 10^{-5} T^2 + 5.793 \times 10^{-2} x_{Mo} T \end{aligned} \tag{3.6}$$

Where T is in K. The valid temperature range is 300 - 800 K.

No initial porosity was assumed in the unirradiated fuel. Therefore, Eq. (3.5) is not intended to be applicable to a porous U-Mo alloy.

Fig. 4 compares the data used for correlation fitting with the model predictions. The predictions are generally close to the data.

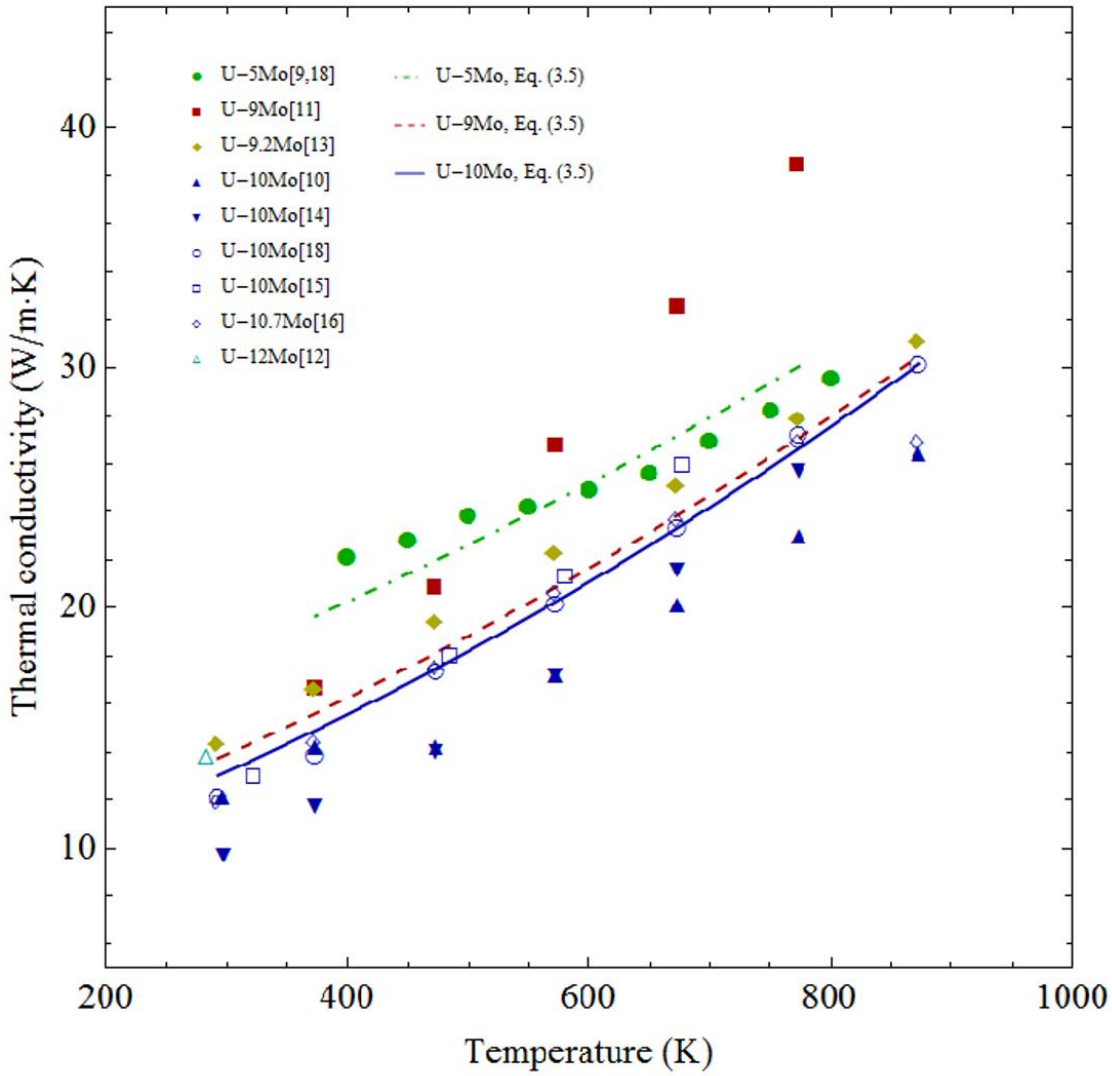

Fig. 4 Measured data and model predictions for unirradiated U-Mo alloys. The number in front of Mo indicate the Mo content in weight percent.

3.5 Thermal conductivity of Aluminum

Aluminum 1060 is used for the matrix material of U-Mo/Al dispersion fuel. Thermal conductivity of aluminum may need to be defined for U-Mo fuel modeling. In the report of Cheon and Kim [20], thermal conductivity of pure aluminum was obtained based on the Touloukian and George and is given in Eq. (3.7) and is shown in Fig. 5.

$$k_{Al}(T) = 254.16 - 0.0435\mathrm{T} \tag{3.7}$$

Where T is in K in the range of $298 \leq \mathrm{T} \leq 933$ K.

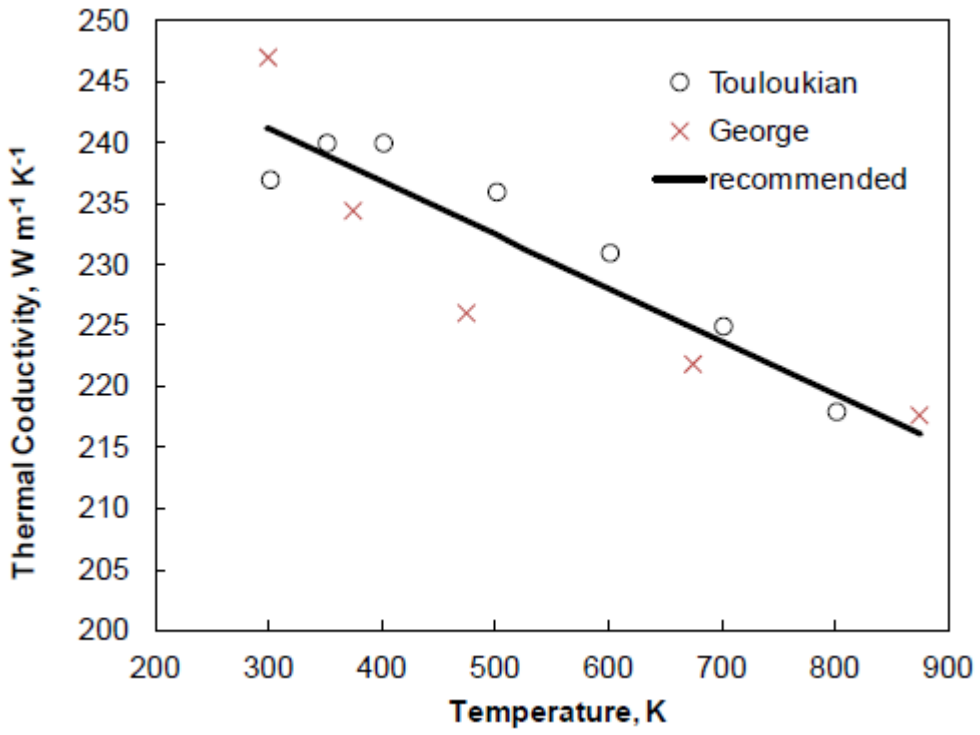

Fig. 5 Thermal conductivity of aluminum

The overall trend of the thermal conductivity decreased with an increase in temperature.

3.6 Comparison of data by S.H. Lee and predictions by Bruggeman model

At first, U10Mo/Al case has been compared with the Bruggeman model that had been calculated with the Eqs. (3.5) and (3.7). The calculation and comparison result are shown in Fig. 6. The thermal conductivity tendencies from the calculation and experiment are different for the cases of 10 vol. % and 30 vol. %.

In the estimation with the model calculation, for low vol. % of U-Mo cases, the conductivity of Al is twenty times greater than that of U-Mo, which makes the overall thermal conductivity tendency decreased as the temperature increases according to the conductivity tendency of Al. But the overall trend became different as the vol. % of U-Mo increase that the thermal conductivity increases with the temperature.

The reason for this different tendency appeared in low particle vol. % cases will be presented in next chapter.

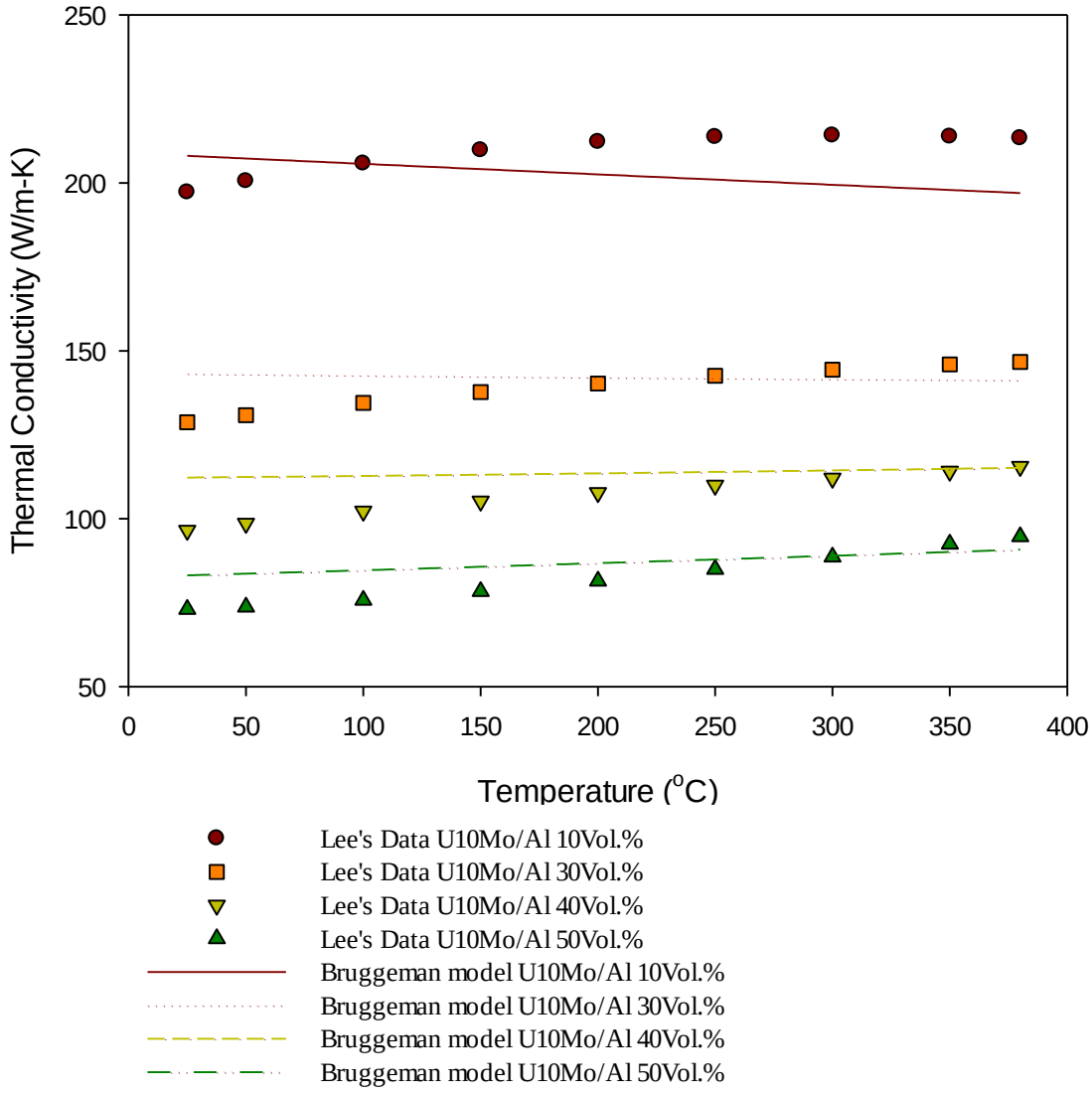

Fig. 6 Comparison Lee's data and Bruggeman model predictions

4. Analysis of the data

4.1 Al thermal conductivity

It is argued that the conductivity of Al increases or decreases as with the temperature increases. The temperature effect became different as Al has high purity. When the impurity exist as a form of a second phase particle in Al matrix, it can be regarded as a composite material to follow thermal behaviors of a general composite. Otherwise, the impurity forms a solid-solution with Al metal as solid-solid lattice, in which the thermal conductivity will decrease. The effect of impurity is significant and the thermal conductivity decreases when the temperature is low. However, the effect became negligible at high temperature. The overall thermal conductivity increases with temperature.

Typically, the thermal conductivity of aluminum is usually increased with the temperature rise. However, the thermal conductivity of Al is likely to decrease over the temperature that is higher than two third of the melting point of pure Al. The thermal conductivity of aluminum decreases significantly when the temperature is near the melting point that is around 923K for the pure aluminum.

Touloukian collected the data of aluminum thermal conductivity and recommended the thermal conductivity of aluminum, as shown in the Figs. 7 and 8. He suggested the thermal conductivity of aluminum which usually increases with the temperature rise but decreases over some temperature.

According to the points which is mentioned above, the recommended thermal conductivity which is suggest by Touloukian [21] is appropriate.

The measured thermal conductivity of U-Mo/Al that will be used in the following section were in a temperature range from the room temperature to 380℃. It is expected that the thermal conductivity of Al generally increases with temperature in this range when we examined the data from Lee's experiment. However, thermal conductivity of Al in Eq. (3.7) modeled by Cheon and Kim was derived with George's data that showed a significant decreasing in thermal conductivity of Al respect to the temperature. It is considered that the data from George [22] was deviated from the general tendency observed by different authors [21, 23, 24], so it is reasonable to employ the thermal conductivity correlation proposed by Touloukian for the prediction.

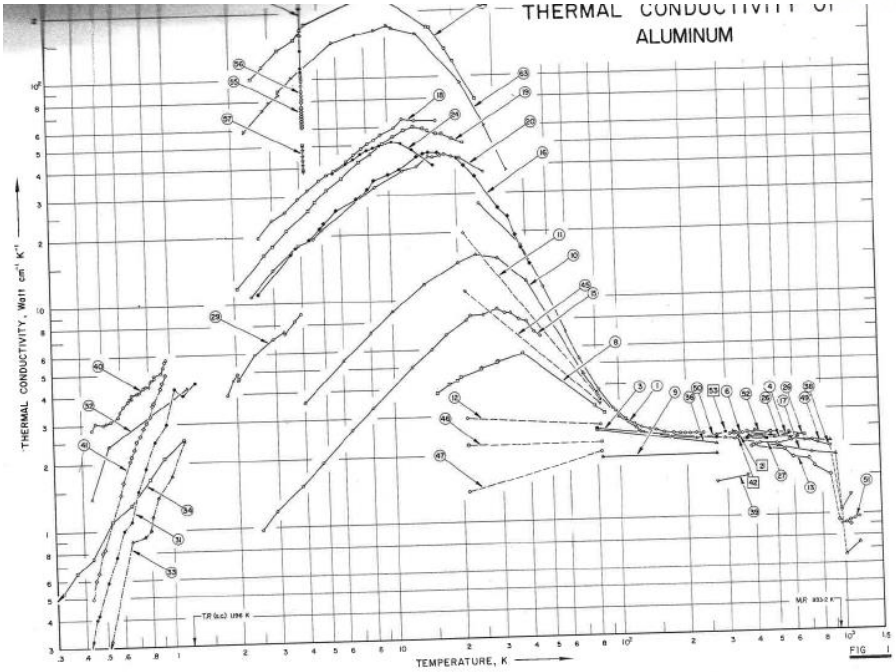

Fig. 7 Thermal conductivity data of Al

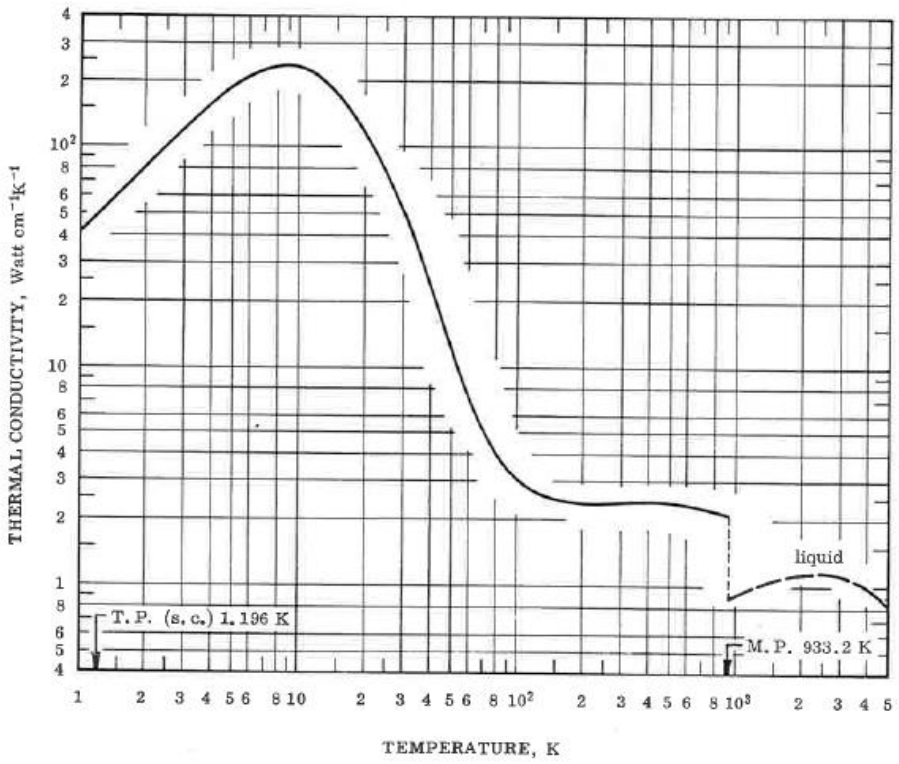

Fig. 8 Recommended value of Touloukian

4.2 Analysis of measured data by S.H. Lee

4.2.1 Review of preparation

The sample has been manufactured by extrusion and this is dispersion fuel. Lee has made it disk-shape. With this sample of 2.5mm thickness, the thermal diffusivity and specific heat capacity has been measured. In old days, the fuel was not compound evenly and the distribution of Al is not uniform. When the sample is produced by extrusion, Al is taken first without mixed if the fraction of Al is large because Al is ductile. When the lower part of the sample is cut, the fraction of Al is large which means the amount of fuel is less. It will be 2% difference or more.

4.2.2 Density correction

Lee used densities of U-Mo/Al dispersion fuel measured at room temperature. However, it is necessary to consider a thermal effect on the density of meat in terms of thermal expansion.

5. New Thermal Conductivity Model for U-Mo/Al Dispersion Fuel

5.1 Modeling of thermal conductivity of pure Al

As explained in chapter 4.1, the recommended thermal conductivity which is suggest by Touloukian is appropriate.

The thermal conductivity of the aluminum is derived using the data in the Table 8. The correlation is given as follows:

$$k_{Al} = -5.19\times10^{-10}T^4 + 1.46\times10^{-6}T^3 - 1.53\times10^{-3}T^2 + 6.52\times10^{-1}T + 144.3 \qquad (5.1)$$

where T is in K.

Further analysis was done using the thermal conductivity from Eq. (5.1).

Table 8 Recommended thermal conductivity of Touloukian

T (K)	Thermal Conductivity (W/m·K)
300	237
350	240
400	240
500	237
600	232
700	226
800	220
900	213
933	211

5.2 Correction of density employed by S.H. Lee

5.2.1 Thermal expansion and density of Aluminum

The correlation of thermal linear expansion of aluminum is obtained by using the interpolation method of experimental data from many authors [25]. Thermal linear expansion of aluminum increase relatively linear shape with the temperature rise as shown in Fig. 9. Aluminum linear expansion is suggested by Touloukian like Table 9, the variation of linear expansion of aluminum is changed to increase and decrease at the 293 K with the variation of temperature.

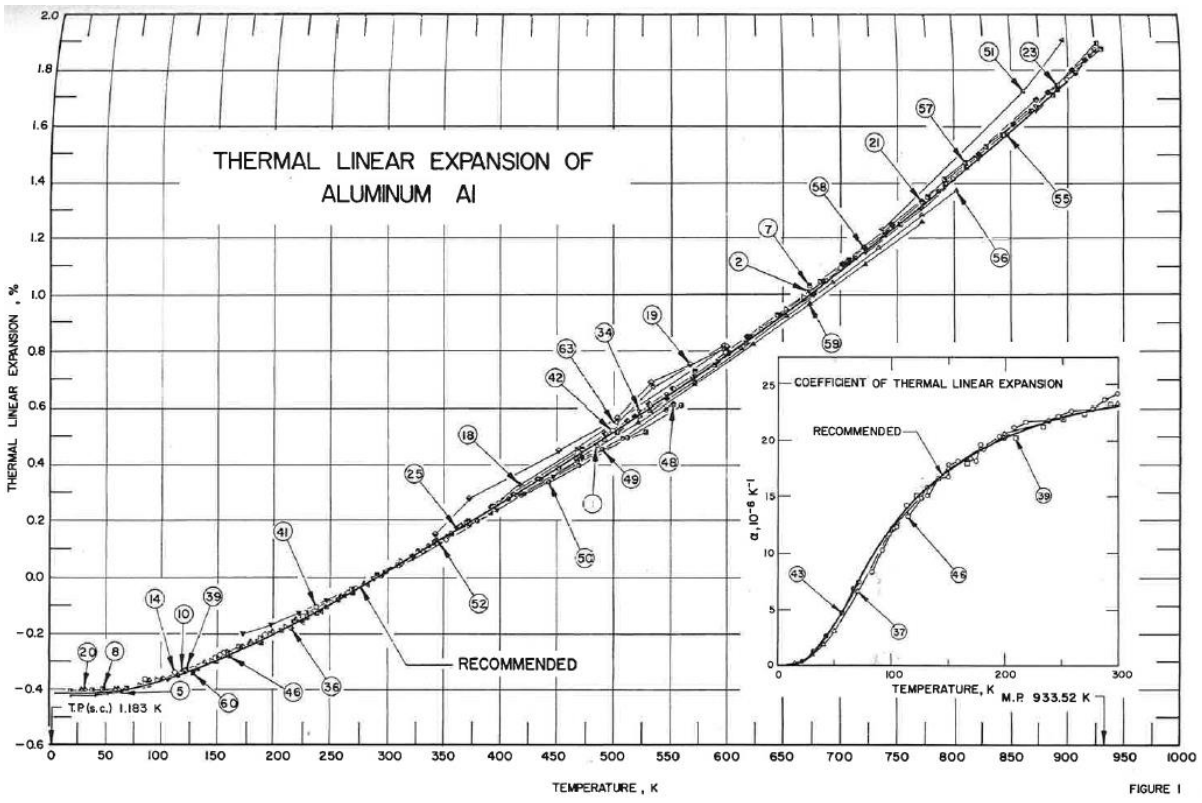

Fig. 9 Thermal linear expansion of Aluminum

Table 9 Recommended values of Touloukian

Temp (K)	Linear Expansion ($\triangle L/L_0$, %)
5	-0.418
50	-0.413
100	-0.371
200	-0.203
293	0.000
400	0.259
500	0.514
600	0.787
700	1.084
800	1.408
900	1.764

The correlation of thermal linear expansion is shown as Eq. (5.2) which is obtained from Touloukian paper.

$$\Delta L / L_0 = 0.018 + 2.364\times10^{-3}(T-300) + 4.164\times10^{-7}(T-300)^2 + 8.270\times10^{-10}(T-300)^3 \quad (5.2)$$

Where T is in K in the range of $300 \leq T \leq 900$ K.

The relationship between density and linear thermal expansion is shown as Eq. (5.3), the value of ρ_0 is 2.7g/cm^3 in the equation.

$$\rho(Al) = \frac{\rho_0}{\left(1+\Delta L / L\right)^3} \quad (5.3)$$

The density of aluminum is calculated by using Eqs. (5.2) and (5.3) which is considered with the thermal expansion, the result of calculation is shown as Table 10.

Table 10 Density of Aluminum

Temp (℃)	Density (g/cm^3)
25	2.70
50	2.69
100	2.68
150	2.67
200	2.66
250	2.65
300	2.64
350	2.63
380	2.63

5.2.2 Thermal expansion and density of U-Mo

Thermal expansion equation for γ-phase U-Mo alloys have been reported by several sources. Thermal expansion of U-Mo is proportional to the temperature regardless of Mo contents. Eq. (5.4) provides the variation in the thermal expansion coefficient with temperature.

$$\alpha_T = 7.91 + 1.21 \times 10^{-2} T \qquad (293 < T < 773K) \qquad (5.4)$$

where T is the temperature in K and α_T is in 10^{-6}/K.

5.2.3 Densities of U-Mo/Al dispersion fuel

The density of U-Mo/Al dispersion fuel was calculated by the following mixture equation :

$$\rho_{U-Mo/Al} = V_{U-Mo}\rho_{U-Mo} + (1 - V_{U-Mo})\rho_{Al} \qquad (5.5)$$

The density of U10Mo/Al dispersion fuel is shown as Table 11 – 13, and the density should be reduced because thermal expansion of material is considered. The density of fuel is increased with the increase of ratio of material which have higher density particle.

Table 11 Density of U10Mo/Al dispersion fuel

Temp (℃)	U10M_A10 (g/cm^3)	U10M_A30 (g/cm^3)	U10M_A40 (g/cm^3)	U10M_A50 (g/cm^3)
25	4.15	7.05	8.50	9.95
50	4.15	7.04	8.49	9.94
100	4.14	7.03	8.48	9.93
150	4.13	7.02	8.47	9.91
200	4.12	7.01	8.45	9.90
250	4.11	6.99	8.44	9.88
300	4.10	6.98	8.42	9.86
350	4.08	6.96	8.40	9.84
380	4.08	6.95	8.39	9.83

Table 12 Density of U8Mo/Al dispersion fuel

Temp (℃)	U8M_A10 (g/cm^3)	U8M_A30 (g/cm^3)	U8M_A40 (g/cm^3)	U8M_A50 (g/cm^3)
25	4.18	7.15	8.63	10.11
50	4.18	7.14	8.62	10.10
100	4.16	7.13	8.61	10.09
150	4.15	7.11	8.59	10.07
200	4.14	7.10	8.57	10.05
250	4.13	7.08	8.56	10.03
300	4.12	7.06	8.54	10.01
350	4.10	7.05	8.52	9.99
380	4.10	7.04	8.51	9.98

Table 13 Density of U6Mo/Al dispersion fuel

Temp (℃)	U6M_A10 (g/cm^3)	U6M_A30 (g/cm^3)	U6M_A40 (g/cm^3)	U6M_A50 (g/cm^3)
25	4.21	7.23	8.74	10.25
50	4.20	7.22	8.73	10.24
100	4.19	7.21	8.72	10.23
150	4.18	7.19	8.70	10.21
200	4.17	7.18	8.69	10.19
250	4.16	7.16	8.67	10.17
300	4.14	7.15	8.65	10.15
350	4.13	7.13	8.63	10.13
380	4.12	7.12	8.62	10.12

5.3 Comparison of density-corrected Lee data and predicted thermal conductivity

Prediction of Bruggeman model is compared with previous calculation, the prediction is calculated by using the data of Lee which is corrected by new density of aluminum with thermal expansion and the new correlation of aluminum thermal conductivity.

The trend of thermal conductivity isn't distinct at the case of low particle volume %, in contrast with the case on the chapter 3.6. But, the experimental data is higher than the value of estimation when the case of 10vol. % U10Mo/Al dispersion fuel and U6Mo 40vol. % and 50vol. %.

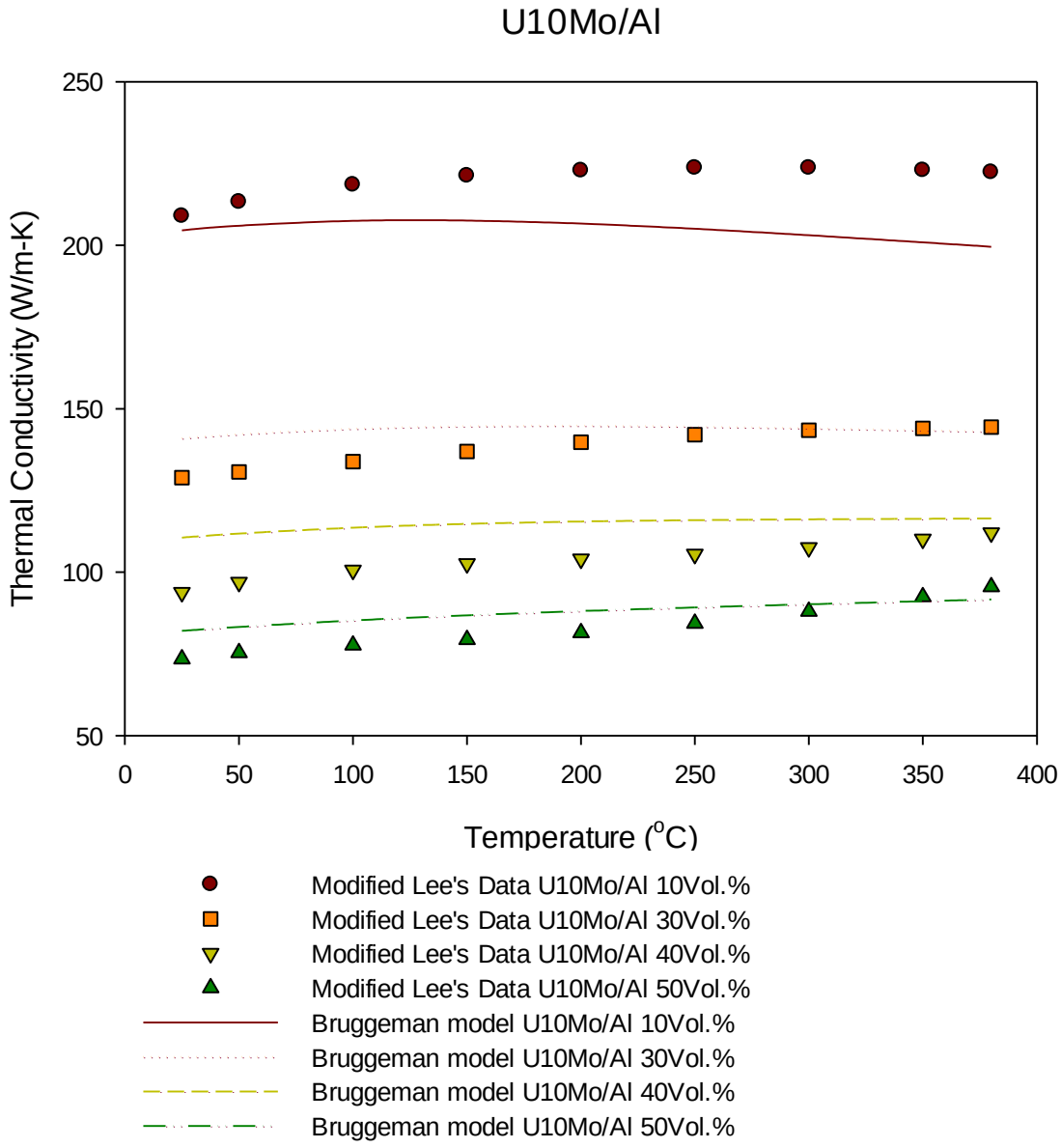

Fig. 10 Modified Lee's Data and Bruggeman model predictions of U10Mo/Al dispersion fuel

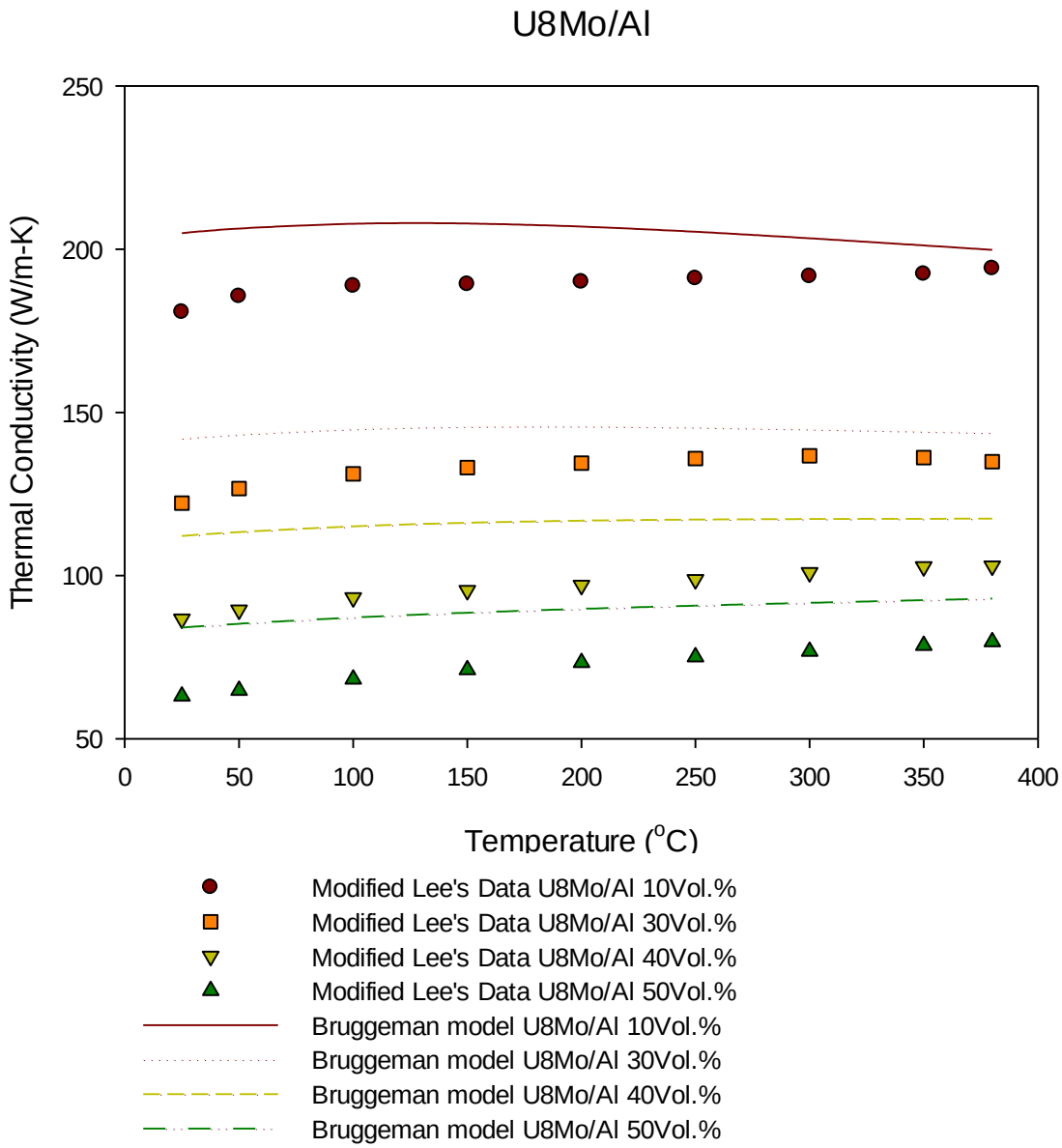

Fig. 11 Modified Lee's Data and Bruggeman model predictions of U8Mo/Al dispersion fuel

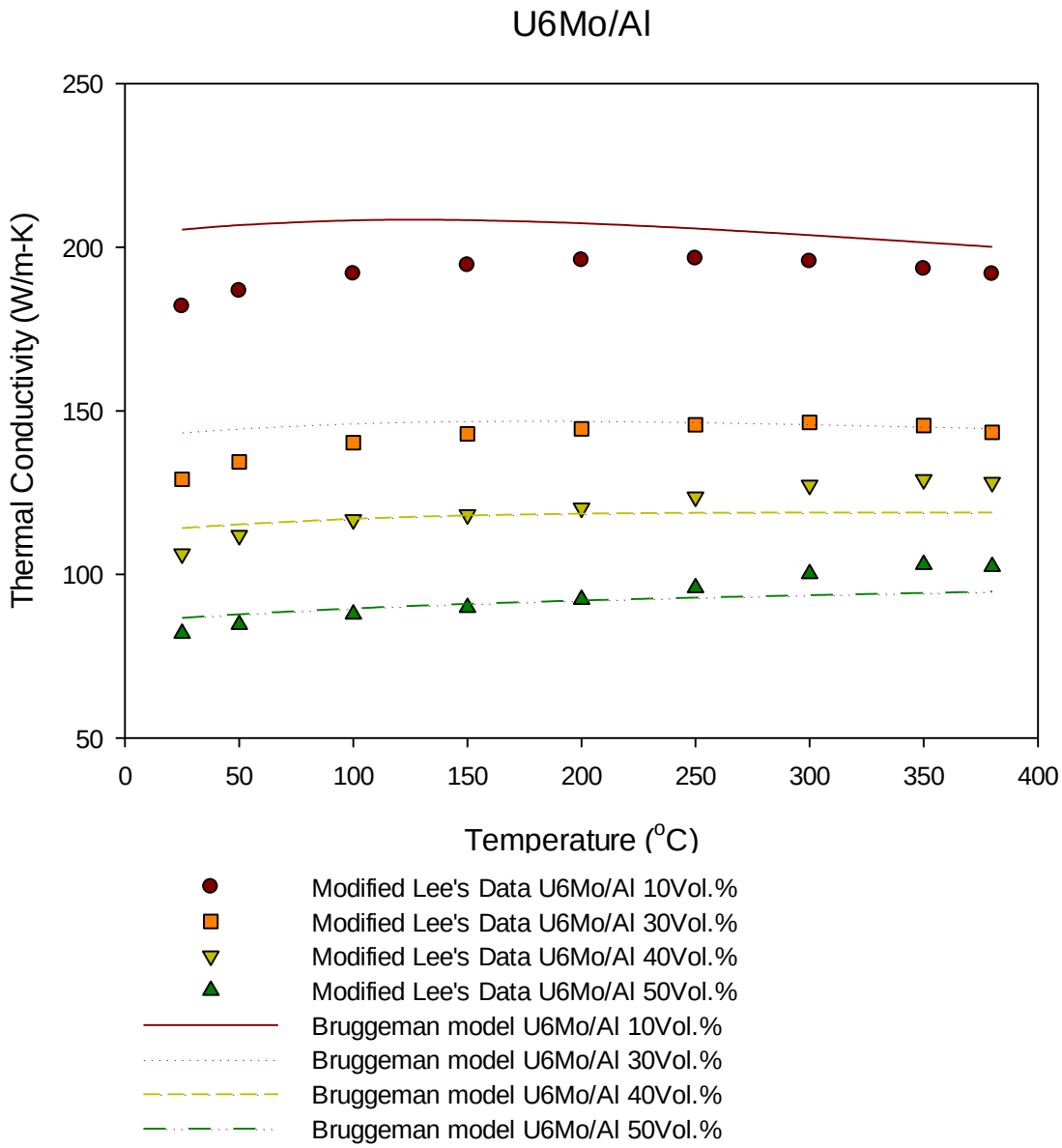

Fig. 12 Modified Lee's Data and Bruggeman model predictions of U6Mo/Al dispersion fuel

5.4 Sample homogeneity

At room temperature, the thermal conductivity of Al matrix is ~20 times higher than that of U-10Mo. Hence, the thermal conductivity of the U-Mo/Al dispersion fuel meat is governed chiefly by Al.

The reason for the generally higher results by the Bruggeman model may be due to the local inhomogeneity of fuel particle distribution. The actual local fuel volume fractions to give the values calculated using the Bruggeman model were estimated as follows:

Table 14 Estimated fuel vol. % of U10Mo/Al dispersion fuel

	Nominal fuel vol.%	Estimated fuel vol.%
U10Mo_A10	10	8.6
U10Mo_A30	30	30.3
U10Mo_A40	40	41.7
U10Mo_A50	50	49.4

During the laser flash sample preparation, the sample size was 2.5 mm. Hence, local fuel particle inhomogeneity occurs. To more accurate measurement, local fuel volume fraction needs to be measured using an SEM image.

Data have been compared from U10Mo/Al, U8Mo/Al, and U6Mo/Al with same volume fraction. Judging from the fact that the thermal conductivity of Mo is less than that of Al, and the difference between the thermal conductivity of U10Mo and U6Mo is not so much, the values from the experiment should be same with same volume fraction.

As it was told above, inhomogeneity will occur while the experiment sample is made. To reduce the inhomogeneity of the sample, research has been performed with the averaged values regarding the experiment data for each volume fraction.

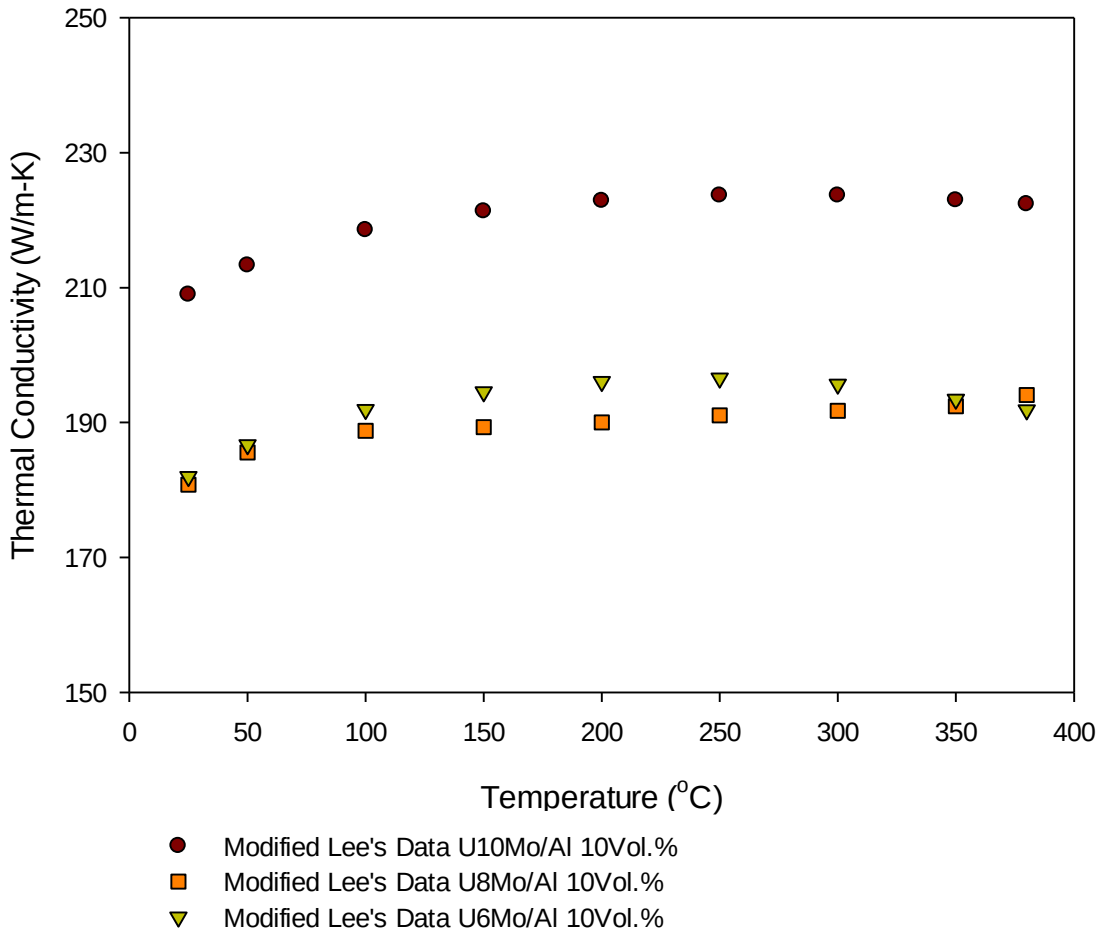

Fig. 13 Thermal conductivities of U-Mo/Al dispersion fuel with 10vol. %

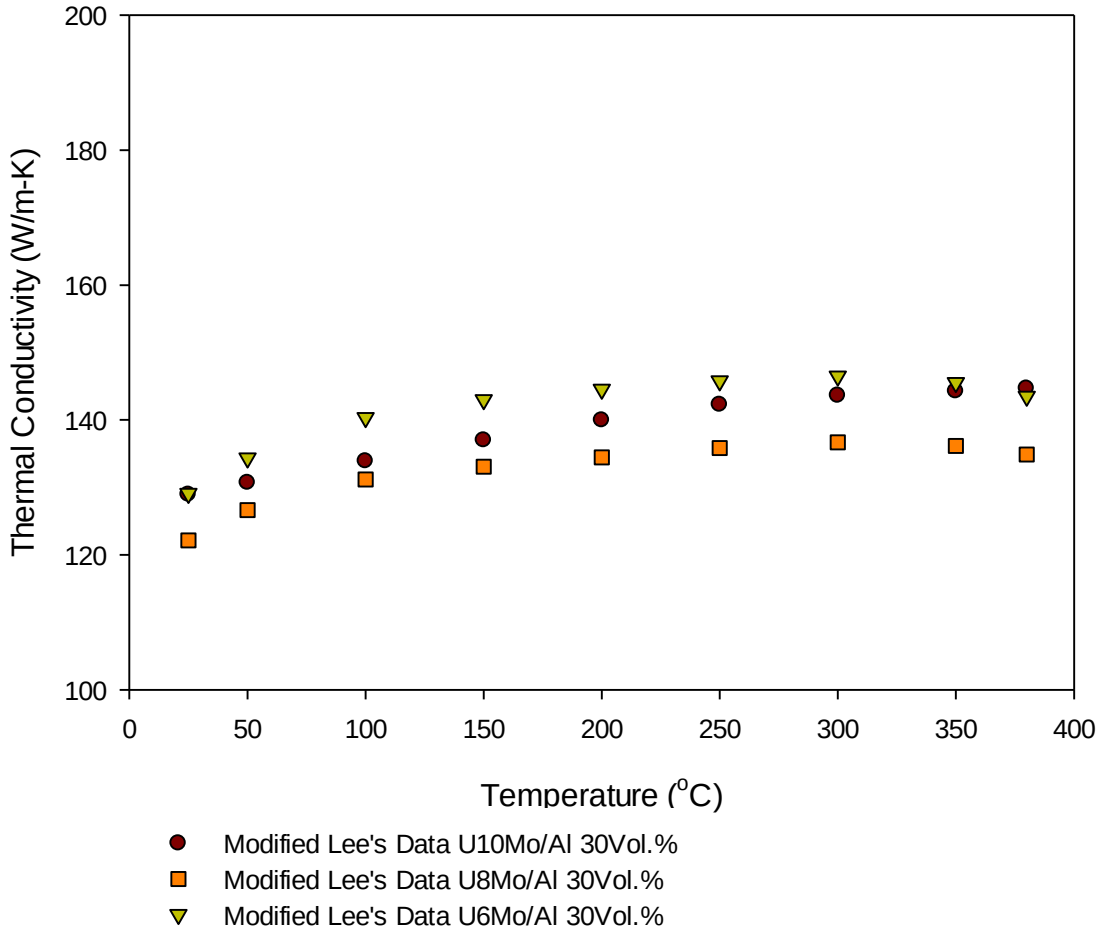

Fig. 14 Thermal conductivities of U-Mo/Al dispersion fuel with 30 vol. %

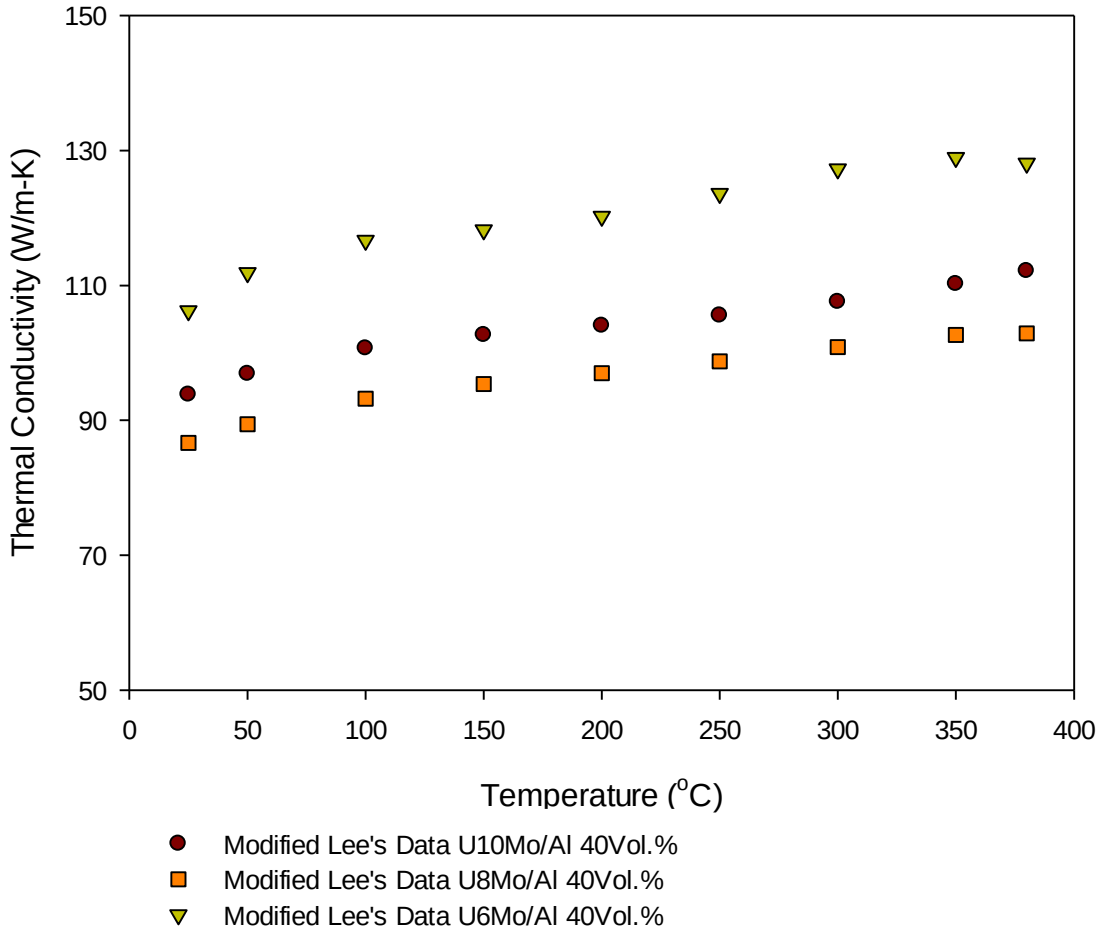

Fig. 15 Thermal conductivities of U-Mo/Al dispersion fuel with 40 vol. %

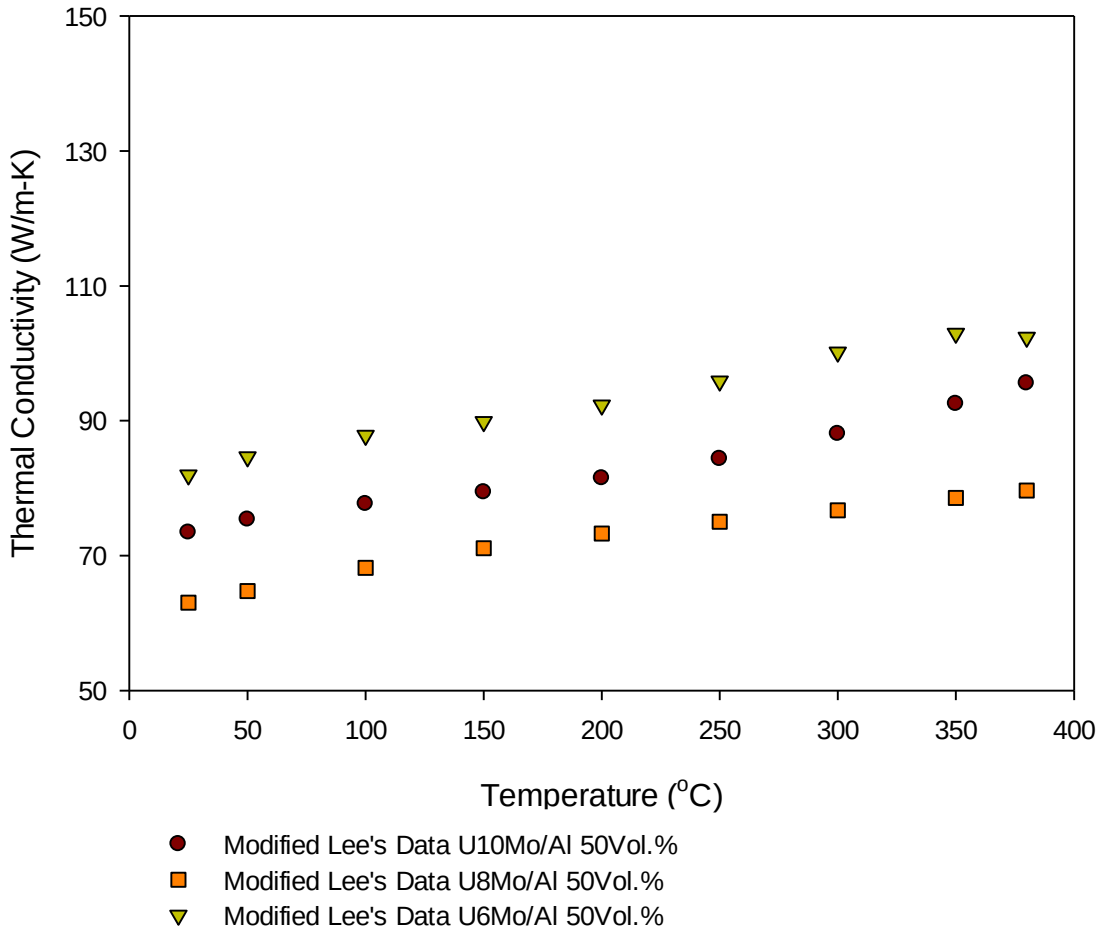

Fig. 16 Thermal conductivities of U-Mo/Al dispersion fuel with 50 vol. %

5.5 Comparison of density-corrected average Lee data and predictions of Bruggeman model

To reduce the effect of local inhomogeneity, measured U-Mo/Al thermal conductivity with same U-Mo volume fraction are averaged locally. It is reasonable since an effect of Mo content on thermal conductivity of U-Mo is not significant. Fig. 17 shows a comparison of Lee's averaged data and the Bruggeman model predictions. It is shown in the Fig. 17 that Bruggeman model predictions overestimate than the experiment results. The effect of poor contact between fuel particles and Al matrix needs to be characterized for more accurate results.

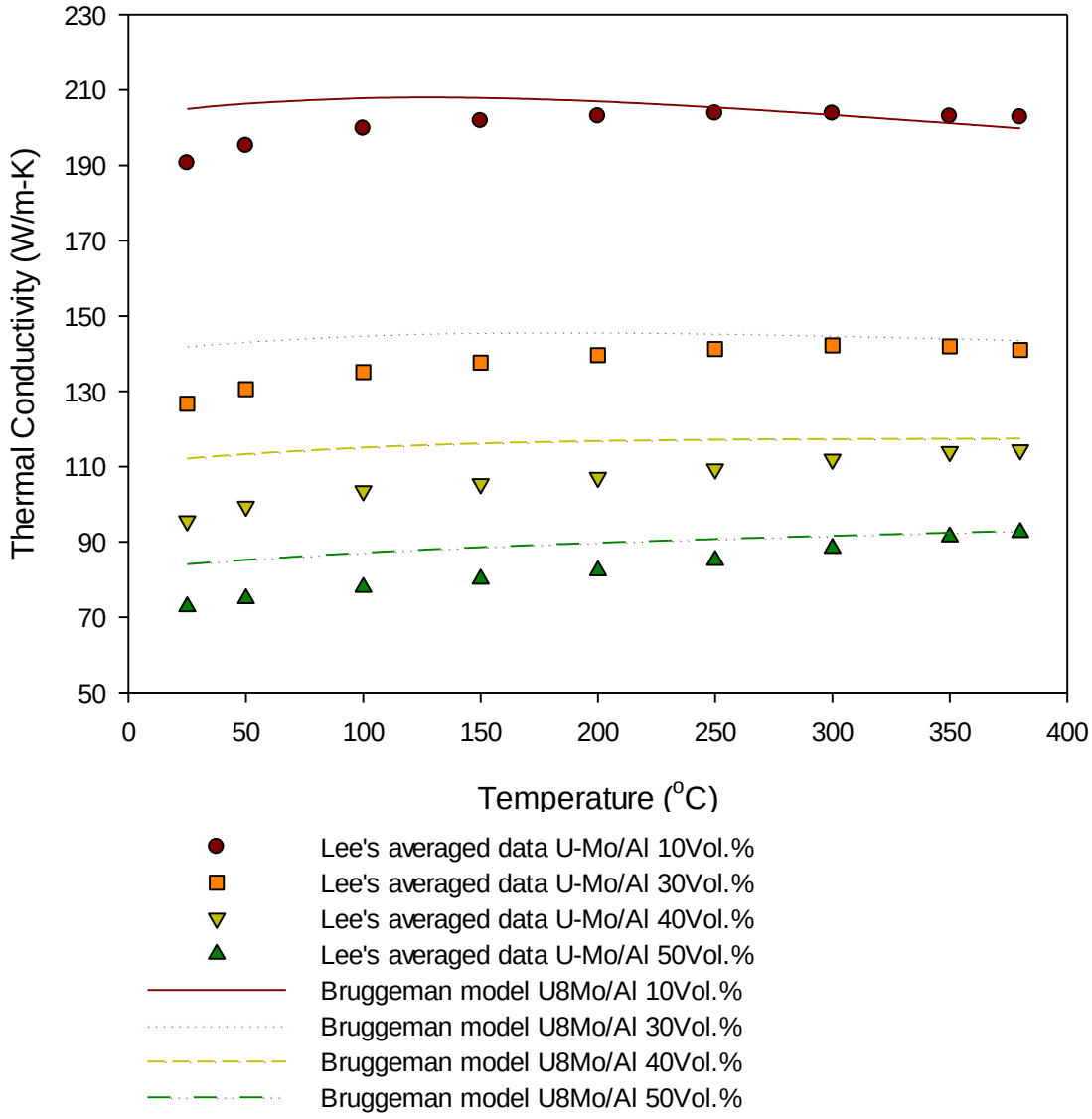

Fig. 17 Comparison of density-corrected Lee's Average Data and Bruggeman model predictions

5.6 Interfacial thermal resistance between U-Mo and Al

The Bruggeman model, as other theoretical models commonly do, assumes perfect contact between the fuel particles and Al matrix.

However, in reality, it is known that a thin oxide layer covers surface of U-Mo particles in Lee's experiment. This oxide layers interfere and make the contact imperfect between the two materials. Hence, a gap occurs from the imperfect contact as shown in Fig. 18. Because of this, the thermal conductivity decrease occurs. And this effect increases as the volume fraction increases.

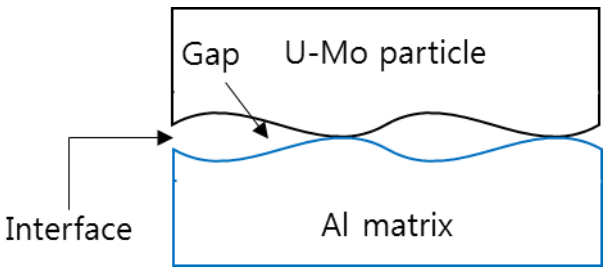

Fig. 18 Contact between U-Mo particle and Al matrix

We defined it 'Surface Thermal Resistance (R_1)' that the resistance between this U-Mo particle and Al matrix.

5.7 Al-Al interfacial resistance

In the model, the matrix is a defect-free monolithic continuum. When we make matrix with melting the pure metal, we can make it almost single crystal. This process will be easier with atomization and slow cooling. Besides, the result will be better with the high thermal conductivity such as Al. Al powder, however, is used for Al matrix in Lee's experiment. Fig. 19 shows a SEM photo of an Al powder typically used at KAERI for meat fabrication.

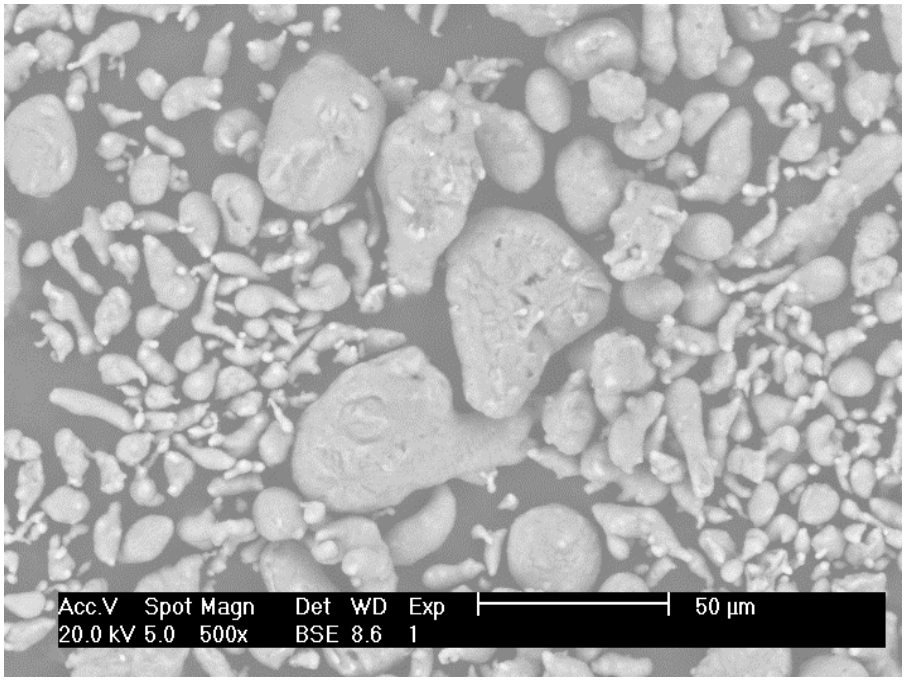

Fig. 19 SEM photo of an Al powder typically used at KAERI for meat fabrication

If a defect or an alloying occurs, a grain can occurs subsequently because Al is metal. When a dislocation is formed due to a mechanical stress or a forging, a grain boundary follows. Fig. 20 is for the Al 6061 matrix made in powder metallurgy (PM) manufacture and it shows that there are many grain boundaries.

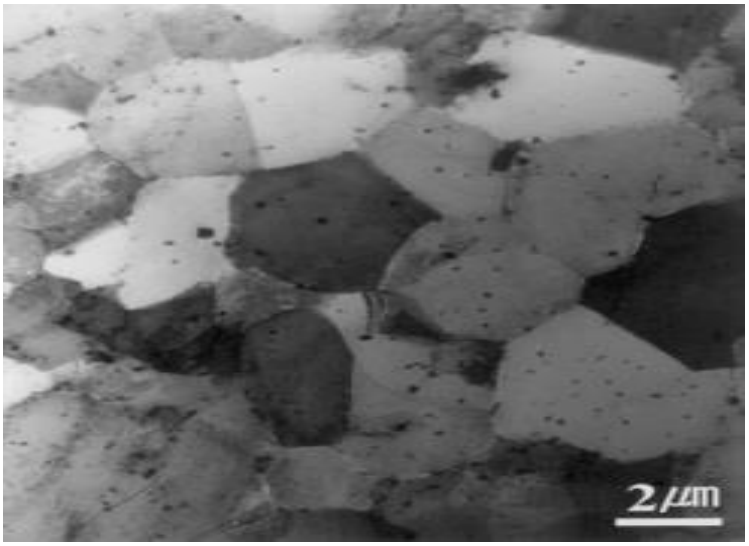

Fig. 20 TEM micrograph of powder-metallurgically made Al [26]

Like this, the defects in Al matrix cause the thermal conductivity reduction. We defined the resistance 'Surface thermal resistance (R_2)' between Al-Al

5.8 New model

The Bruggeman model, as other theoretical models commonly do, assumes perfect contact between the fuel particles and Al matrix. The matrix is a defect-free monolithic continuum. However, in reality, it is known that a thin oxide layer covers surface of U-Mo particles, and Al matrix has some defects such as dislocation, grain boundaries, cracks and so on.

The thermal resistance factor was introduced in order to complement the limitations assumed in Bruggeman. This factor considered not only the resistance between U-Mo particles and Al matrix but also resistance in Al matrix.

The effect of porosity in the dispersion fuel was not considered because the power made by atomization method showed almost a full density ($P < 0.01$) after a hot extrusion [27].

The new model was developed by expanding the Bruggeman model with a new factor, which is the surface thermal resistance factor. The equation is as follows.

$$k_e = \frac{1}{4}\left[A + \left(A^2 + 8k_1^* k_2^* \right)^{\frac{1}{2}} \right] \tag{5.1}$$

$$A = \left(3\nu_1 - 1\right)k_1^* + (3\nu_2 - 1)k_2^* \tag{5.2}$$

$$k_n^* = k_n(1-\alpha_n) \tag{5.3}$$

$$\alpha_n = \frac{R_n k_n}{r_n} \tag{5.4}$$

$$R_n = a_n\left[1 - \exp(-\frac{b_n}{T})\right] \tag{5.5}$$

where,

k_e = Effective thermal conductivity (W/m·K)

k_1 = Thermal conductivity of U-Mo particle (W/m·K)

k_2 = Thermal conductivity of Al (W/m·K)

ν_1 = Volume fraction of U-Mo particles

ν_2 = Volume fraction of Al

R_n = Surface thermal resistance (m^2K/W)

r_n = Radius of particle (m)

T = Temperature (K)

α_n = Surface thermal resistance factor

a_n, b_n = Constant

The new factor, alpha, is given as a function of surface thermal resistance, thermal conductivity and particle size of the particle. The surface thermal resistance is a function of two constants and temperature. Two constants are obtained by best fitting with Lee's average data.

Here, n is 1 for U-Mo case or 2 for Al case, a_1=0.01, b_1 = 0.01, a_2 = 0.005, and b_2 = 0.0002.

5.9 Comparison of density-corrected average Lee data and predictions of new model

It has been compared for the developed model and Lee's averaged data which decreases inhomogeneity of samples. It is noticeable that newly developed model gives more accurate prediction compared to the previous model.

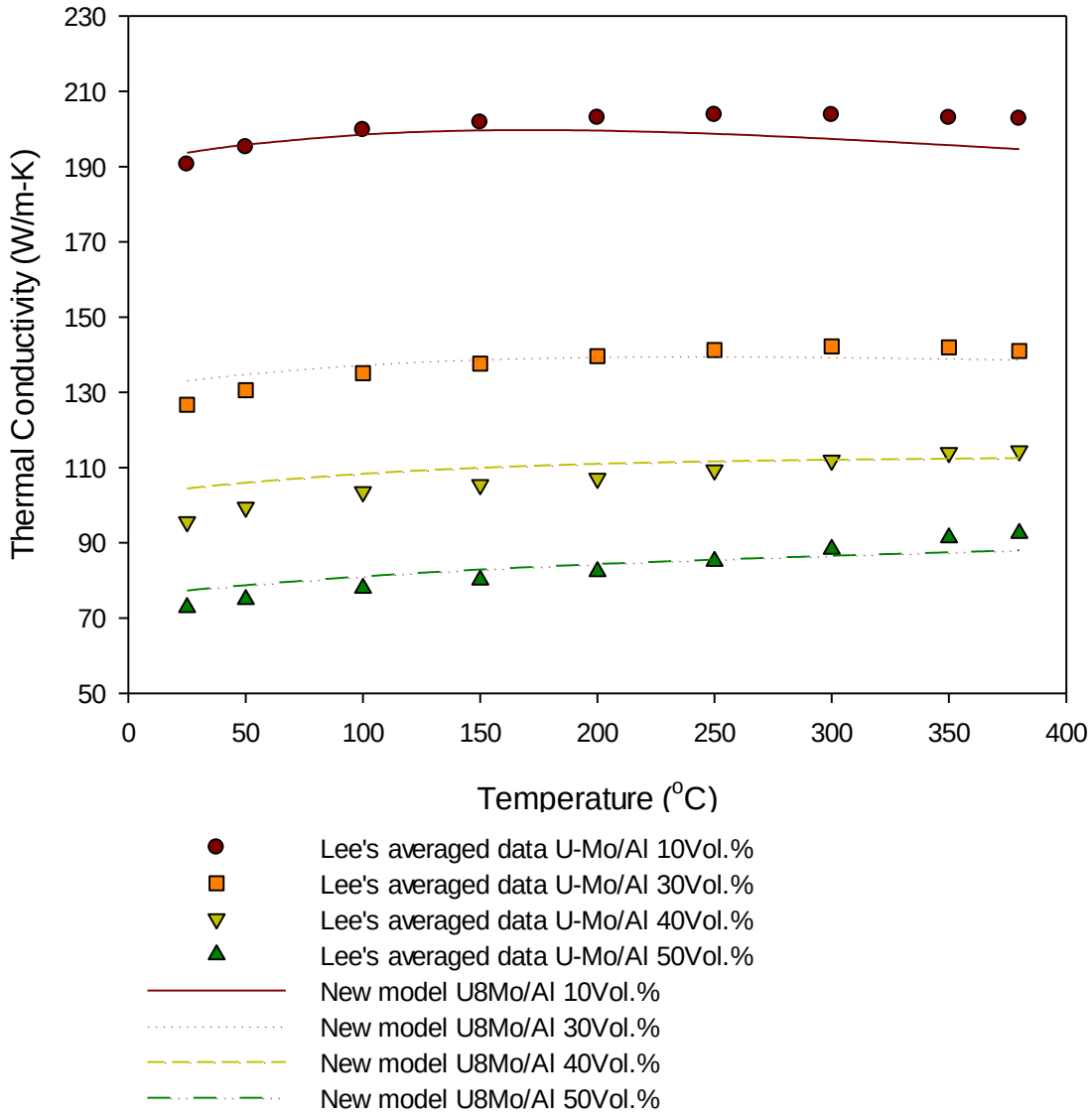

Fig. 21 Comparison of density-corrected Lee's Average Data and New model Predictions

6. Sensitivity Study

The KOMO-4 irradiation test performed at KAERI, South Korea, contained U–Mo/Al–Si, where the Si contents are 0, 2, 5, and 8 wt. %, dispersion fuel with 5.0 g U/cm^3 U loadings and was tested in the HANARO reactor. The test samples are 200-mm long rodlets composed of fuel meat with radius 3.2 mm directly bonded to Al-1060 cladding with thickness 0.76 mm [28].

Here the effect from the difference between Lee's experimental data and Bruggemen model prediction value with the linear power histories of KOMO-4 test sample. In Lee's experiment, U8Mo/Al 30vol. % has been used for its similarity to the KOMO-4 test sample (U7Mo/Al 32.7 vol. %) based on the same Uranium loading. The linear power of KOMO-4 is 92 kW/m without irradiation effect at BOL and the cladding surface temperature is 119℃.

To calculate the centerline temperature of fuel meat, following two equations are used. Outer Temperatures of cladding and meat were calculated using Eq. (6.1). Centerline temperature of the fuel meat was calculated with Eq. (6.2).

$$T_1 = T_2 + q \times \frac{\ln(\frac{r_2}{r_1})}{2\pi kL} \tag{6.1}$$

$$T(r) = \frac{q''' r_0^2}{4k}\left(1 - \frac{r^2}{r_0^2}\right) + T_s \tag{6.2}$$

Table 15 Centerline temperature and thermal conductivity of fuel meat (KOMO-4 Case)

U8Mo/Al 30 vol.% case	T meat, c (℃)	K_{meat} (W/m·K)
L, case	178.6	139.0
R, w/o case	176.2	145.8
R, case	178.5	139.3

L, case : Using modified Lee's averaged data

R,w/o case : Using thermal conductivity without surface thermal resistance. (Bruggeman model)

R, case : Using confirmed surface resistances of U-Mo, and Al. (New model)

The result showed about 2.4℃ between L, case and R, w/o case. 2.4℃ difference has no effect because the center temperature of UO_2 reach 1000℃ in case of LWR fuel. In research reactor fuel, however, this difference should not be ignored because the fuel center temperature is 180℃. Especially, this would have effect on interaction layer production and fuel swelling that are the significant problem for research reactor fuel.

7. Conclusions

A new thermal conductivity model that is applicable to U-Mo/Al dispersion fuel has been developed. The new model comprises the following:

1. The thermal conductivity of Al as a function of temperature was developed using the recommended data by Touloukian.

2. Lee's experimental data were revised using temperature-dependent densities of U-Mo fuel and Al matrix in the sample.

3. The interfacial thermal resistance between the U-Mo particles and Al matrix was considered. In addition, the grain boundary effect in the Al matrix was taken into account.

The newly developed model more accurately predicted the thermal conductivity of U-Mo/Al meat than the existing Bruggeman model.

References

[1] S. H. Lee, J. M. Park, and C. K. Kim, "Thermophysical Properties of U–Mo/Al Alloy Dispersion Fuel Meats," *International Journal of Thermophysics*, vol. 28, pp. 1578-1594, 2007.

[2] J. C. Maxwell, *A Treatise on Electricity and Magnetism, .* Dover Publications, Inc., 1904.

[3] D. A. G. Bruggeman, "Dielectric constant and conductivity of mixtures of isotropic materials," *Ann. Phys.*, pp. 636-664, 1935.

[4] Z. Hashin and S. Shtrikman, "A variational approach to the theory of the effective magnetic permeability of multiphase materials," *Journal of applied Physics*, vol. 33, pp. 3125-3131, 1962.

[5] S. Durmaz, "A numerical study on the effective thermal conductivity of composite materials," 2004.

[6] A. E. Powers, "Conductivity in aggregates," Mar. 6 1961.

[7] D. P. H. Hasselman and L. F. Johnson, "Effective Thermal Conductivity of Composites with Interfacial Thermal Barrier Resistance," *Journal of Composite Materials 21* pp. 508-515, 1987.

[8] R. E. Taylor, "Thermophysical Properties of U-Mo Core," 2000.

[9] J. Rest, Y. S. Kim, G. L. Hofman, M. K. Meyer, and S. L. Hayes, "U-Mo Fuels Handbook," Argonne National Laboratory2009.

[10] Y. S. Kim and G. Hofman, *AAA fuels handbook*: United States. Department of Energy, 2003.

[11] J. L. Klein, "Uranium and It's Alloys," 1962.

[12] S. Konobeevsky, A. Zaimovsky, B. Levitsky, Y. Sokursky, N. Chebotarev, Y. Bobkov, *et al.*, "Some physical properties of uranium, plutonium, and their alloys," in *Proceedings of the second UN international conference on the peaceful uses of atomic energy, paper P/2230*, 1958.

[13] S. H. Lee, "An Investigation of the Thermophysical Properties of U-Mo Dispersion Fuel Meats," in *Proceedings of the RERTR Meeting, Las Vegas, Nevada*, 2000.

[14] T. Matsui, T. Natsume, and K. Naito, "Heat capacity measurements of $U_{0.80}Zr_{0.20}$ and $U_{0.80}Mo_{0.20}$ alloys from room temperature to 1300 K," *Journal of Nuclear Materials*, vol. 167, pp. 152-159, 9// 1989.

[15] R. McGeary, "Development and Properties of Uranium-Base Alloys Corrosion Resistant in High-Temperature Water," *Pt. I., Alloys Without Protective Cladding, WAPD-127*, 1955.

[16] C. Roy, A. Radenac, and F. Cado, "Conductivité thermique d'un alliage d'uranium à 10% en poids de molybdène entre 320 K et 680 K," *Journal of Nuclear Materials,* vol. 48, pp. 369-371, 10// 1973.

[17] H. A. Saller, R. F. Dickerson, A. A. Bauer, and N. E. Daniel, "Properties of a Fissium-type Alloy," Battelle Memorial Inst., Columbus, Ohio1956.

[18] Y. Takahashi, M. Yamawaki, and K. Yamamoto, "Thermophysical properties of uranium-zirconium alloys," *Journal of Nuclear Materials,* vol. 154, pp. 141-144, 6// 1988.

[19] Y. Touloukian, R. Powell, C. Ho, and P. Klemens, "Thermophysical Properties of Matter-The TPRC Data Series. Volume 1. Thermal Conductivity-Metallic Elements and Alloys," DTIC Document1970.

[20] J. S. Cheon and Y. S. Kim, "Material Properties of Aluminum Alloys and Pure Zirconium for Use in High-density Fuel Development for Research Reactors," Nuclear Engineering Division, Argonne National Laboratory2012.

[21] Y. S. Touloukian, "TPRC Data for thermal conductivity," 1970.

[22] G. E. Totten and D. S. MacKenzie, *Handbook of Aluminum: Vol. 1: Physical Metallurgy and Processes* vol. 1: CRC Press, 2003.

[23] S. Abu-Eishah, "Correlations for the thermal conductivity of metals as a function of temperature," *International journal of thermophysics,* vol. 22, pp. 1855-1868, 2001.

[24] R. Powell, C. Y. Ho, and P. E. Liley, "Thermal conductivity of selected materials," DTIC Document1966.

[25] Y. S. Touloukian, "TPRC Data for thermal expansion," 1975.

[26] W. J. Kim, S. H. Hong, and J. H. Lee, "Superplasticity in PM 6061 Al alloy and elimination of strengthening effect by reinforcement in superplastic PM aluminum composites," *Materials Science and Engineering: A,* vol. 298, pp. 166-173, 2001.

[27] H. J. Ryu, Y. S. Kim, J. M. Park, H. T. Chae, and C. K. Kim, "Performance evaluation of U-Mo/Al dispersion fuel by considering a fuel-matrix interaction," *Nuclear Engineering and Technology,* vol. 40, 2008.

[28] Y. S. Kim, J. M. Park, H. J. Ryu, Y. H. Jung, and G. Hofman, "Reduced interaction layer growth of U–Mo dispersion in Al–Si," *Journal of Nuclear Materials,* vol. 430, pp. 50-57, 2012.

Acknowledgments

First of all, I would like to express my deepest gratitude to my advisor, Professor Dong-Seong Sohn, for giving me the opportunity generous support, encouragement with patience, and guidance for my research work. I am also truly grateful to co-advisor, Dr. Yeon Soo Kim for providing valuable data, constant inspiration, and helpful comments given to me during the course. I would like to appreciate him greatly for valuable discussions based on his expertise and theoretical basics to my research field.

I would also like to thank my committee members Professor Ji Hyun Kim, Professor In Cheol Bang for their valuable time and thoughtful insight.

In addition, I appreciate Dr. Jong Man Park and Dr. Sang Hyun Lee for permitting for us to use their data and support for our research.

I wish to special thanks to our group members of “INFUEL”, who helped me during the course leading to a master’s degree: Je Kyun Baek, Gwan Yoon Jeong, Cheol Min Lee, Tae Won Cho, Ji Hyeon Kim, Mi Jin Kim, Hee Jae Lee, Young Jin Kim, Joo Young Lie. I wish you all the best for your work and would be always be happy to hear good news.

I give my sincere thanks to my colleagues in UNIST: Seung Won Lee, Dong Han Yoo, Jeong Seok Park, Sang Hoon Shin, Jong Jin Kim, Ju Ang Jung, Sung Dae Park, Sarah Kang, Tae Woo Tak, Sang Il, Choi, Kyoung Joon Choi.

Many friends have helped me stay here through this difficult time. Their support, encouraging comments, and a lot of prayer helped me overcome difficulties. I deeply appreciate them.

Last, but foremost, I would like to appreciate my parents, my sister, and all of my family for their endless love, understanding, and support.